WSRC-MS-2001-00672 Rev. 1

Characterization of Confined Pinch Welds in Type 304L Stainless Steel

By

P. S. Korinko
Westinghouse Savannah River Company
Savannah River Site
Aiken, SC

M. J. Pechersky

D. J. Zecha, Jr.

G. J. McKinney

L. Riester
Oak Ridge National Laboratory
Oak Ridge TN

P. J. Blau
Oak Ridge National Laboratory
Oak Ridge TN

E. Lara-Curzio
Oak Ridge National Laboratory
Oak Ridge TN

A document prepared for TRENDS IN WELDING RESEARCH at Pine Mountain, GA, USA from 4-15-2002 to 4-20-2002.

DOE Contract No. **DE-AC09-96SR18500**

Characterization of Confined Pinch Welds in Type 304L Stainless Steel

P. S. Korinko*, M. J. Pechersky*, D. J. Zecha*, Jr., G. J. McKinney*,
L. Riester, P. J. Blau**, E. Lara-Curzio**,**
*Westinghouse Savannah River Company, Aiken, SC
**Oak Ridge National Laboratory, Oak Ridge TN
WSRC-MS-2001-00672

Abstract

Efforts have been undertaken to characterize the stresses induced in resistance pinch welds used to seal vessels which contain high pressure radioactive gasses. Subsequent to the weld a costly and time consuming process, known as hot air decontamination (HAD) is used to remove the radioactive gasses that are entrained in the weld and surrounding metal. A process to replace HAD is under development. To qualify this new process it must be shown that the mechanical and physical properties of the weld are substantially the same as those using HAD.. These properties include the weld microstructure and the residual stresses in the vicinity of the weld. The method of making pinch welds is first described as well as one cutting method. The methods of characterizing the weld and a comparison between cut and uncut specimens by several characterization methods are presented.

Introduction

Westinghouse Savannah River Company uses resistance pinch welds to close vessels filled with tritium which is a radioactive isotope of hydrogen. The vessel is filled through a small diameter tube referred to as a stem and the stem is then pinch welded shut while still under pressure to seal the gas inside of the vessel. This process results in tritium becoming entrained in the weld metal and heated metal adjacent to the weld. This surface and near surface contamination results in off-gassing which is unacceptable for the storage of these vessels. The contamination is currently removed using a process of blowing hot air onto the surface and relying on the localized heating and diffusion to remove the contamination from the metal. This hot air decontamination (HAD) process is both time consuming and costly.

It was recognized that a significant cost savings could be achieved if the HAD process could be eliminated. The concept to eliminate HAD is to cut the fill stem within the weld from the nubbin which is the portion that attaches to the fill manifold. It is envisioned that this cut location will decrease the size of the contaminated region that is off-gassing. A further cost reduction is possible if the new process could also eliminate the generation of metal fines such as those made when the stems are cut and filed. The confined pinch welds also develop small metal extrusions, "ears", during welding where the electrodes and confinement dies meet, Fig. 1. The fill stem of the vessel must also be cut from the nubbin. This step will decrease the amount of contaminated waste generated. A shearing and coining device was conceived that would accomplish these goals, i.e., eliminate HAD and not generate metal fines.

In order to implement the device, a study was undertaken to examine alternatives to the shearing device that may accomplish some, but not all of the goals. These alternatives include using either a precision saw cut which would eliminate HAD but still generate fines and a precision end mill which has the same shortcomings. The first phase of this study was to pare down the large number of evaluation tools that are available. Based on input from the designers of the vessels and leading technical experts, residual stresses and their impact on the vessel integrity were of prime concern. The vessel reliability was also a consideration since it is possible for the weld process to produce closure lengths that range from 2.5 mm (0.100") to 4.6 mm (0.180"). The fill stems are also made from three different alloys that can be either forged or simple bar stock. The effects of the closure length and bond integrity using the new cutting method needed to be evaluated. To address all these concerns a phased study was devised.

In Phase 1, one alloy, type 304L stainless steel (SS), was selected. The weld conditions that produced closure lengths that ranged from the minimum to the maximum requirements were established. Test samples were then made under the conditions that should produce the most annealed weld; these samples were tested in either the as-welded or end-milled condition using numerous methods to evaluate residual stresses. The methods proposed were: metallographic examination, microhardness testing, nanoindentation testing, laser fringe interferometry, X-ray diffraction, neutron diffraction, and boiling magnesium chloride stress corrosion cracking. The best methods were carried forward for Phase 2 using type 304L SS in which welds cut using the other two processes and welded at other conditions will be examined. Phase 3 will be used to examine type 316L SS and alloy Nitronic 40 (21-6-9) with closure lengths that run the gamut and the pared down cutting and evaluation methods. It is the intent of this paper to discuss methods and results of the Phase 1 activities, not including X-ray or neutron diffraction.

Weld Conditions

Resistance pinch welding for fill stem closure is a specialized application that is used to close tritium containing vessels. The welds that were evaluated for this study were made using a confining die so the welded diameter perpendicular to the pinch direction is nominally the same as the original diameter. This is accomplished using the device shown in Fig. 1. The welding process is such that the fill stem attached to the vessel is placed into the weld fixture, the vessel filled,

and the weld sequence initiated. The study welds were made by evacuating the stem and system, introducing 2 atm of deuterium, clamping the tube with the appropriate force, verifying the resistance, then applying the current. The force, voltage, and current were measured using a computerized data acquisition system (DAS). The weld energy was then calculated.

Type 304L SS forged fill stems and type 304L SS tubing pieces were used to establish the weld conditions that produced closure lengths from the minimum to the maximum allowable. The weld quality requirement also includes the absence of weld expulsions, also known as spits, and splits, absence of bonding at the end of the pinch weld. Weld expulsion occurs when the weld conditions are too hot and a significant amount of metal is melted. The splits often occur when the weld is too cold. These weld defects are determined as part of the X-ray evaluation for closure length. A typical weld expulsion is shown in Fig. 2.

Fig. 1. Weld fixture for confined pinch welds.

The weld conditions that were evaluated to determine the full range of weld parameters (current and force on the welding electrodes) that would produce welds from the minimum closure to the maximum closure without weld defects are shown in Fig. 3. The closed triangles indicate closure welds that do not meet minimum requirements, the circles indicate welds with expulsions, while the solid diamonds indicate welds that meet the radiography requirements. It is evident that a wide range of weld conditions can produce acceptable welds. The weld conditions vary from 3100 A at 5115 N (1150 lbs) to 3950 A and 6005 N (1350 lbs). This window encompasses the production process. In addition, the welds for testing were all made with 2 atm of deuterium in the internal volume.

Weld conditions for Phase 1 included only welds made at the lower right corner of the process window. These welds are expected to be the "hottest" condition. As such, they should be the most annealed. It is subsequently expected that these welds will exhibit the greatest change in incremental residual stress for the various cutting processes, thus making them ideal samples for Phase 1. The subsequent phases of the testing will use welds made at the nominal conditions and the other three corners of the weld parameter window to determine residual stresses.

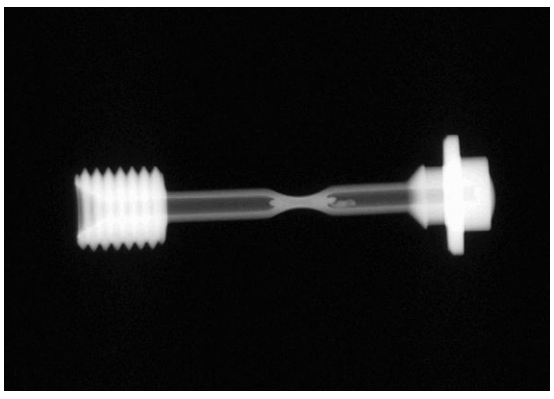

Fig. 2. Weld radiograph showing expulsion on right side of weld and nubbin to the left.

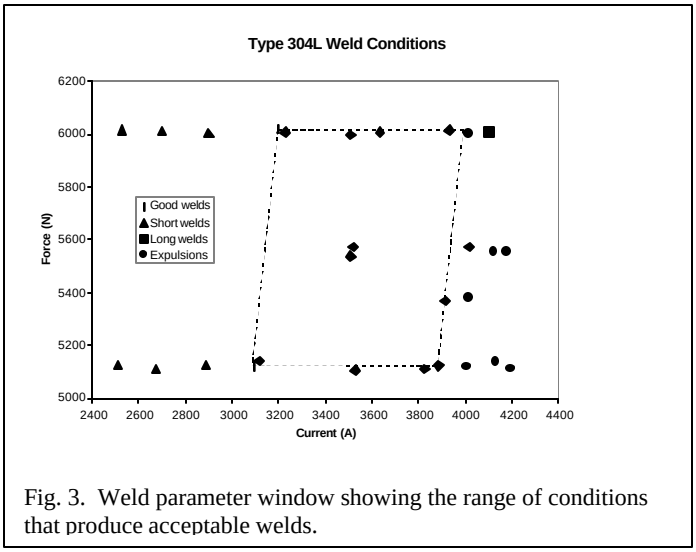

Fig. 3. Weld parameter window showing the range of conditions that produce acceptable welds.

Experimental Procedure

Metallographic Examination was conducted by cutting the stems parallel to the axis using an electro-discharge machine (EDM). The samples were mounted in epoxy, ground and polished. Samples were electrolytically etched with 10% oxalic acid. The samples were then examined on either a light or electron optical microscope. The amount of damage caused by the cutting process was of primary interest, although other attributes were included, to determine impact on service behavior.

Microhardness Testing was performed on mounted and polished samples. The hardness profiles were used not only to characterize the properties across the weld and in other regions of interest but also to determine if changes in local hardness could be measured. The Knoop hardness indenter, a 50 g load, and a dwell time of five seconds were used. The hardness indentations were placed as close to the edge as possible. The nearest approach was about 100 μm.

Nanoindentation testing was conducted to determine if the observations from the metallographic examination and microhardness testing could be better quantified. The nanoindentation was conducted at the Oak Ridge National Laboratory (ORNL) using a Nanoindentater II™. A Berkovich indenter and a total displacement of 1000 nm corresponding to a load of approximately 60 mN were used for the testing. The loading, holding and unloading data were collected. From these data, the sample stiffness, modulus and hardness were determined. Hardness traverses were made from the cut surface inward at a spacing of approximately 15 nm and at various positions in the weld to characterize the weld properties.

Laser speckle interferometry was conducted at the Savannah River Site (SRS) to determine if the residual stresses could be determined for the cut and uncut stems. This method uses an infrared laser for relieving stress in a small spot (1,2). A dab of temperature indicating paint is applied to the spot and a specklegram of the spot and the surrounding area is captured. The temperature indicating paint spot diameter can range from about 1 mm to 4 mm. A surrounding area of

about 2 cm in diameter is normally captured in the specklegram. The paint is then heated with a laser until it melts. The heat is transferred from the paint into the material resulting in a small amount of localized stress relief as the yield stress of the material drops below the stress levels surrounding the spot. Once the spot and area around it have cooled a second specklegram is captured and the images are processed to determine the in-plane strain. The amount of stress relief depends on the final temperature attained as indicated by the thermal paint since yield stress is a function of temperature.

Magnesium chloride testing was conducted similarly to ASTM G-36 (3), although no calibration curves have been established, thus making the test qualitative. Samples were sectioned longitudinally using the EDM and lightly polished to remove the recast layer. Samples were subsequently cleaned and placed into flasks that had been filled with the appropriate concentration of $MgCl_2$ in water. Samples were visually examined periodically. Photographs were taken in addition to descriptions of the samples being written. The samples were exposed for a total of 12 days. Water was added to the solution to maintain the desired boiling point. The temperature varied by about five degrees Celsius due to evaporation.

Results and Discussion

Metallographic Examination was conducted on fill stems that were welded using the low force, high current weld, i.e., hot conditions, described above. All of the samples were radiographed to determine the weld quality and closure length. Samples were subsequently examined metallographically. The samples were cut longitudinally using EDM.

Typical macrophotographs of the as-welded and end-milled samples are shown in Fig. 4. The stems were plug welded using gas tungsten arc welds (GTAW). This weld, as well as the pinch weld, is visible in Fig. 4. The end-milled sample clearly shows that some of the pinch weld has been removed, as was desired. The as-welded sample exhibits a small amount of extrusion on both the vessel (right) and nubbin (left) side of the weld. The weld geometry, i.e., extrusion and closure length, for both of these samples is acceptable.

The condition near the center of the pinch welds is shown in Fig. 5. There is a small amount of melting at the original interface. These welds would be considered acceptable for service.

A high magnification image, Fig. 6, of the cut edge of the end-milled sample shows a small amount of deformation as evidenced by the change in direction of the metal flow lines. The depth of disturbed metal is approximately 10 μm, a fairly small amount of damage.

Microhardness testing revealed no significant differences in hardness on a traverse initiated near the cut surface and that progressed inwards. A comparison of the hardness profiles in the welded and end-milled region compared to the tube base metal is shown in Fig 7. There is some scatter in the data for the base metal which has hardness values that range from 2.2 to 2.7 GPa. The expected increase in surface hardness based on the cold work induced by end milling the sample was not observed. This result is not unexpected since the scanning electron microscopy (SEM) and metallographic examination indicated that the metal was only disturbed to a depth of 10 μm and the closest that an indentation was made on the cut was 76 μm from the edge. This indicates that the scale of the cutting damage is sufficiently small such that there should be no discernable affect on the product side of the pinch weld.

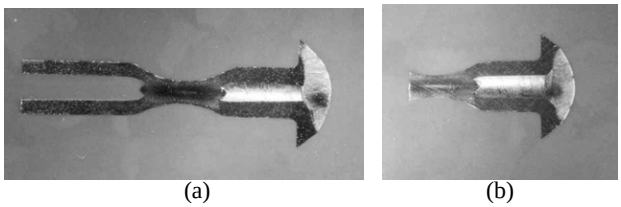

(a) (b)

Fig. 4. Micrographs showing (a) as-welded and (b) end-milled samples.

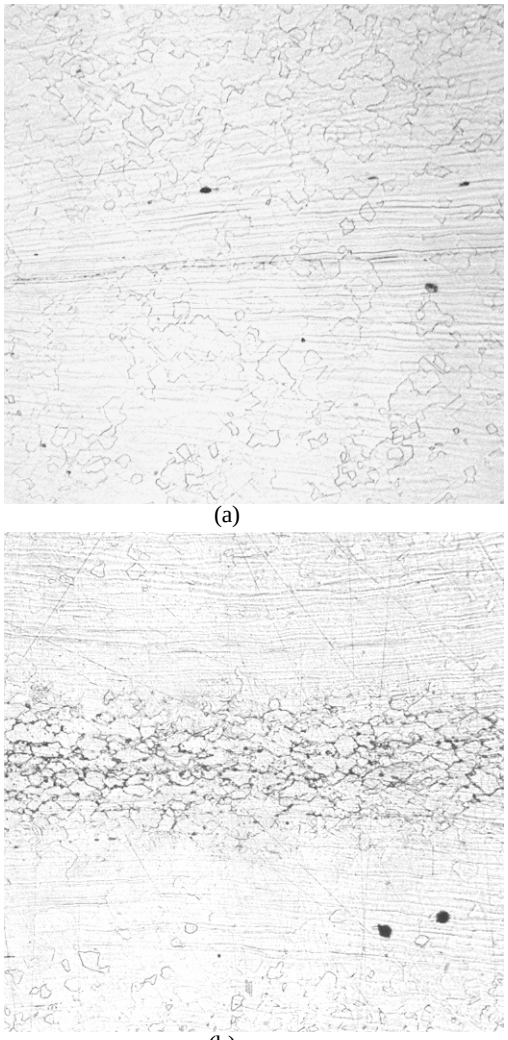

(a)

(b)

Fig. 5. High magnification images of two samples at the weld center line (a) as-welded (b) end-milled.

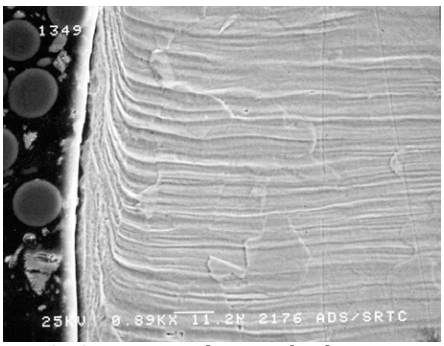

Fig. 6. SEM image showing the damage caused by end milling

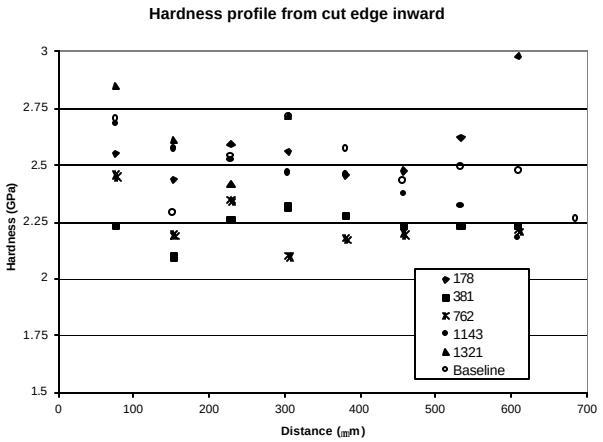

Fig. 7. Microhardness profile of end-milled pinch weld at several elevations.

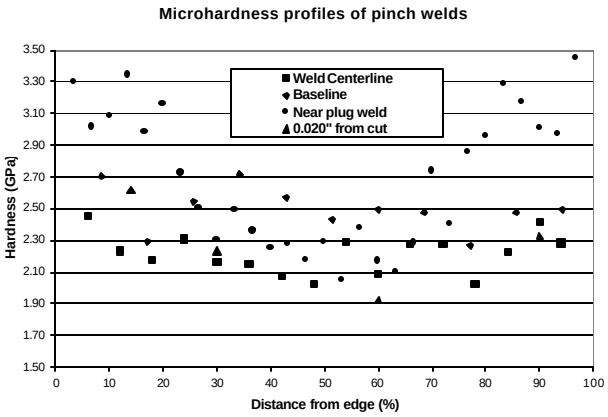

Fig. 8. Microhardness profiles for an end-milled pinch weld sample at three positions in the pinch weld.

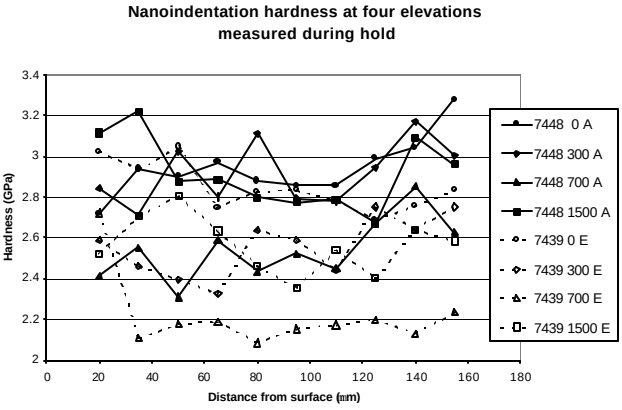

Fig. 9. Nanoindentation hardness profile for as-welded (7448 # A) and end-milled (7439 # E) pinch welds where the # is the distance (elevation) from one edge.

In order to better understand the scatter of the data near the cut portion of the pinch weld, the welds and stems were further characterized using microhardness tests to determine what effect the pinch weld process may have had on the stem properties. As would be expected, the weld process increases the hardness of the stem material where it is cold worked. As an example, the microhardness profile across the weld in three positions for the sample shown in Fig. 8 exhibits an increase in microhardness at the surface followed by a reduction as one progresses into the weld. The hardness is lowest at the weld interface (i.e., 50% of the thickness). The hardness trough is most evident for the location identified as the "near plug weld". This hardness profile also demonstrates that the hardness depends on the axial location. The hardness is lowest at the weld centerline, which is the region that is exposed to the greatest heat due to stem contact resistance.

Nanoindentation testing was conducted to determine if the observations from the metallographic examination and microhardness testing could be better quantified. The near surface indentation was made at approximately 20 nm. This depth is closer than that achieved by microhardness testing but still beyond the disturbed metal shown in Fig. 6. The hardness profiles, Fig. 9, do not exhibit a significant change as the indents progress inward into the weld. The hardness profiles at the outer edges of the weld, i.e., elevations of 0 and 1500 μm, exhibit the highest hardness, as was observed in the microhardness testing. The weld centerline (approximately 700 μm) exhibits the lowest hardness value for both the sample that was end-milled and for the sample in the as-welded condition. The location between the center and edge exhibits an intermediate hardness. The testing of the weld perpendicular to the interface revealed a similar trend with peaks near both edges. Typical profiles for as-welded and end-milled samples are shown in Fig. 10. The trough behavior is also observed. The hardness values are also similar. There is more scatter in the nanoindentation hardness data than in the microhardness data. This can possibly be attributed to sample preparation, since it is well known that surface asperities and roughness contribute to irreproducible results in nanoindentation testing. The samples that were tested had been etched electrolytically with oxalic acid to improve contrast; however, as a consequence, the surfaces exhibited some amount of surface roughness.

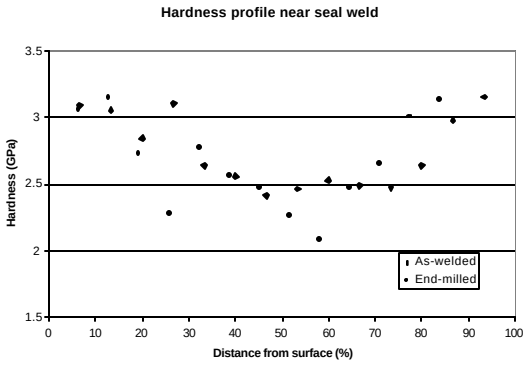

Fig. 10. Nanoindentation hardness profile using nanoindentation through the pinch weld near the plug end.

The nanoindentation testing appears more likely to be useful to discern differences between the cutting methods, especially if the cutting method induces additional damage to the surface that can be seen metallographically. It appears though, that the damage from the cutting using an end mill was confined to a fairly narrow region just below the surface of the cut, the depth of this damage is smaller than the nearest surface indentation that can be made. Nanoindentation, with its

smaller indentation size and the capability of testing nearer the surface, should be useful to test other cutting methods that produce increased depths of damage.

Laser speckle interferometry (1,2) was used as a screening tool to determine if there was an observable change in the residual stress due to cutting. The method was successful in providing data that suggest there is a change due to the cutting. Information is ascertained based on the change in number of fringes between cut and uncut stems. The series of photographs in Fig. 11 demonstrate results of the technique.

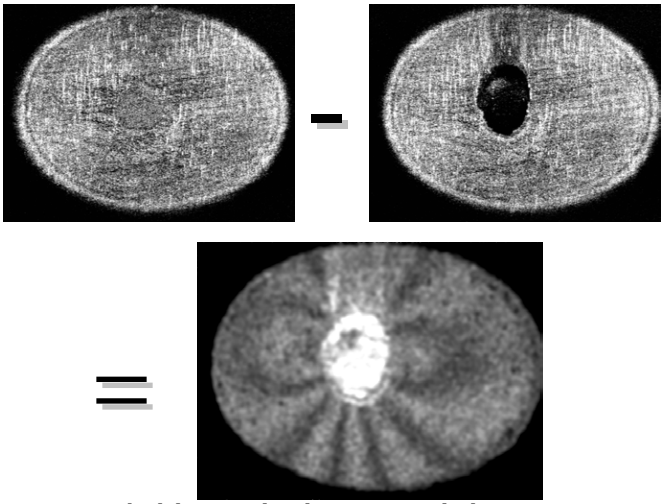

Fig. 11. Methodology used to determine residual stresses using specklegrams and deformation fringes.

The white light photograph in Fig. 12 shows the baseline condition of the stems, which have been painted with a thermal paint. This paint melts when the CO_2 laser beam impinges on it. The residual stresses at this time are then relieved in the localized region of heating. After the stem is fully cooled, a final specklegram is captured and the images processed. The results of the processing are also shown in Fig. 12. There is a difference of one interference fringe between the end-milled and as-welded samples. The residual stress difference due to this count difference has not been quantified and is expected to be completed in a follow-on task.

An improvement of the technique was proposed so that smaller increments of the yield stress could be determined. In the general technique, residual stresses in excess of 80% of the yield were needed for resolution. However, by acquiring images immediately after heating allows residual stresses of about 50% or less of the yield stress to be measured. In addition, a priori knowledge of the yield stress of the material being tested is not required. This situation arises because the system is calibrated and any new constants are determined empirically. These attributes can be more easily seen by considering the governing equations for both methods.

$$s = s_Y + A \times \frac{L}{d} Ee + B \times \frac{d}{L} Ea\Delta T \qquad (1)$$

where:
σ_Y is the yield stress at the elevated temperature, T_H;
L is the distance over which the strain is averaged;
d is the diameter of the heated spot, which is the actual area for which σ is determined;
E is Young's modulus;
α is the coefficient of thermal expansion;

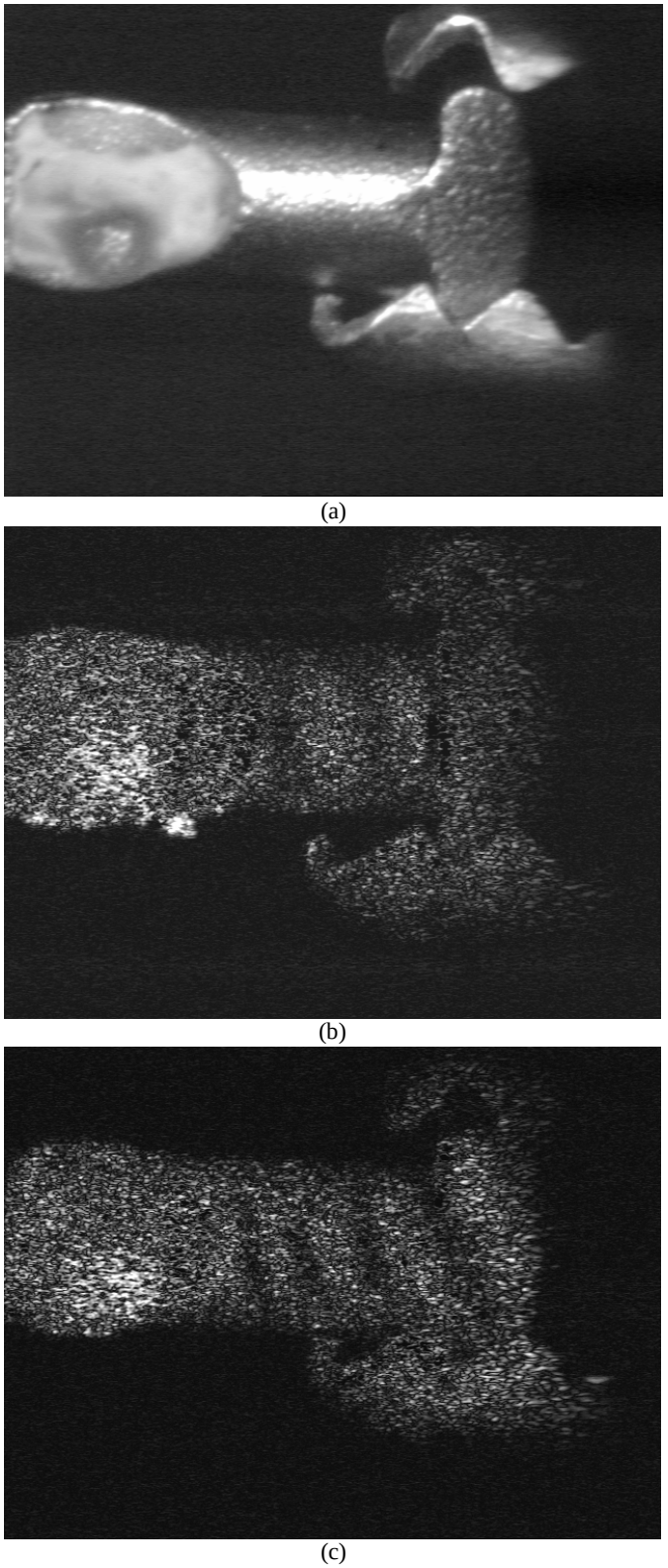

(a)

(b)

(c)

Fig. 12. Laser speckle interferograms showing the (a) white light image (b) an as-welded stem and (c) and an end-milled stem.

ΔT is the temperature rise ($T_H - T_L$), T_L being the initial temperature, and A and B are empirically determined coefficients.

$$s = A_D \times \frac{E E_H}{E - E_H} \cdot 2e - B_D \times \frac{E E_H}{E - E_H} \cdot \frac{d}{L - d} \cdot a \Delta T \qquad (2)$$

Where: E_H is Young's modulus when evaluated at the elevated temperature; A_D and B_D are empirically deteminded coefficeints for this particular equation and the remaining terms have been defined previously. Notice that there is no need to cause plastic deformation to obtain a result. This is a crucial improvement since the yield stress of a specimen is often not known. That is, even if the material is known the amount of work hardening or annealing as a result of joining processes is not generally known. On the other hand, Young's modulus is fairly insensitive to these factors.

Boiling magnesium chloride testing was used at 105 to 140°C. The samples all cracked after exposure at various times to the solutions at these temperatures. The time to cracking was slightly shorter on average for the end-milled samples compared to the as-welded sample. Cracks were observed in the cold deformed area of the weld, i.e., between the weld bead and the edge of the radius for the electrode. The typical post test condition for samples tested at 120°C is shown in Fig. 13. The cracks in the tube wall are clearly evident. These cracks occurred after 3 days for both the as-welded and the end-milled conditions. The time to crack for four crack types on the interior of the tube and three on the exterior is shown in Table 1. On average, there were more cracks in the cut samples than in the as-welded samples.

Table 1. Cracks in as-welded and end-milled pinch welds after exposure in boiling $MgCl_2$ at 120°C.

Crack Type	End-Milled	As-Welded
1	1 day 1 sample	None observed
2	3, 8, 9 days one each day	3, 8 days
3	3 days	None observed
b	8 days	8 days 2 samples
b	1 day	None observed
No cracks	None	Two samples

Internal Cracks

Type 1 - Within the weld electrode imprint (depression) and at the bond line, **Type 2** - Within the weld electrode imprint (depression) but outside the bond line, **Type 3** - At or near the edge of the electrode imprint, **Type 4** - Internal cracks a large distance from the weld impression, **Type 5** - Internal cracks associated with cut surface

External cracks

Type a - At the edge or just outside the weld depression, **Type b** - Within the weld electrode imprint area and in the confining anvils, perpendicular to the tube axis, **Type c** - Circumferential cracks associate with tube depressions at some distance from the weld

(a) (b)

Fig. 13. Type 2 cracks observed in (a) as pinch welded and (b) end-milled test samples.

Summary

The effort to date to qualify a new method of fill stem cutting has been concentrated on weld parameter window verification and weld characterization. This paper described the weld window and indicated the parameters that met the design requirements for type 304L SS. In addition, the conditions that produced unacceptable welds by being too cold, i.e., inadequate closure lengths, and conditions that produced weld unacceptable welds by being too hot, i.e., excessive closure length or weld expulsions, were defined. A number of characterization techniques were used to determine the method(s) best suited for measuring the effect of end-milling on the mechanical properties of the weld. Metallographic examination remains a powerful method to examine surface processing related damage. Microhardness may be useful to examine damage that extends a considerable depth into the surface. Nanoindentation techniques can be used to determine damage that is less severe than that observed by microhardness, yet the depth of disturbed metal was less than the nearest surface approach. Laser speckle interferometry appears to be a useful tool to determine residual stresses. The advent of the improved technique which permits measurement of samples without having prior knowledge of the yield stress of the region of interest appears promising. Boiling $MgCl_2$ testing can be used as screening tool to determine relative differences in stress. The residual stresses in the tubes after welding are significant. A series of calibration tests for the boiling $MgCl_2$ could be used to quantify the stresses. Efforts to determine the residual stresses in pinch welds using X-ray and neutron diffraction are continuing.

Acknowledgements

Numerous people at SRS and ORNL assisted with this research, including E. Estochen, Z. Nelson, C. Foreman, J. Mickalonis, and K. Hicks. This Research sponsored in part by the Assistant Secretary for Energy Efficiency and Renewable Energy, Office of Transportation Technologies, as part of the High Temperature Materials Laboratory User Program, Oak Ridge National Laboratory, Managed by UT-Battelle, LLC, for the U.S. Department of Energy under contract number DE-AC05-00OR22725. The research was also sponsored by Westinghouse Savannah River Company for the U.S. Department of Energy under Contract DE-AC09-96SR18500.

References

1. M. J. Pechersky, E. G. Estochen, and C. S. Vikram, "Enhanced Measurement of Residual Stress by Speckle Correlation Interferometry and Local Heat Treating for Low Stress Levels", Proceedings of ASME PVP 2001: 2001 ASME Pressure Vessels and Piping Conference, Atlanta, Georgia, 22-26 July 2001, ASME.
2. Pechersky, Martin J., Chandra S. Vikram, Determination of Residual Stresses by Local Annealing and Laser Speckle Pattern Interferometry. Post Conference Proceedings of the 1997 SEM Spring Conference on Experimental Mechanics, Society of Experimental Mechanics(1997), pages 116 – 120.
3. ASTM G 36 – 94, Standard Practice for Evaluating Stress Corrosion Cracking Resistance of Metals and Alloys in a Boiling Magnesium Chloride Solution, ASTM, West Conshohocken, PA, USA, 2000.